

# Allan Deviation Computations of a Linear Frequency Synthesizer System Using Frequency Domain Techniques

Andy Wu  
The Aerospace Corporation  
El Segundo, California

## Abstract

*Allan Deviation computations of linear frequency synthesizer systems have been reported previously using real-time simulations. Even though it takes less time compared with the actual measurement, it is still very time consuming to compute the Allan Deviation for long sample times with the desired confidence level. Also noises, such as flicker phase noise and flicker frequency noise, can not be simulated precisely. The use of frequency domain techniques can overcome these drawbacks. In this paper the system error model of a fictitious linear frequency synthesizer is developed and its performance using a Cesium (Cs) atomic frequency standard (AFS) as a reference is evaluated using frequency domain techniques. For a linear timing system, the power spectral density at the system output can be computed with known system transfer functions and known power spectral densities from the input noise sources. The resulting power spectral density can then be used to compute the Allan Variance at the system output. Sensitivities of the Allan Variance at the system output to each of its independent input noises are obtained, and they are valuable for design trade-off and trouble-shooting.*

## 1. Introduction

A fictitious linear frequency synthesizer is used in this analysis. The system generates a system output frequency from a reference Cs Atomic Frequency Standard (AFS) operating at a different frequency. The system block diagram is shown in Figure 1. A reference epoch is generated every 1.5 s based on the AFS frequency and another 1.5 s interval system epoch is generated by the system clock, a voltage control crystal oscillator (VCXO). Both epochs are input to the Phase Meter (PM), and the PM computes the timing error between them. Based on the timing error value, the loop adjusts the phase of the VCXO-generated epoch, so that the VCXO is phase-locked to the reference AFS.

In this paper the system error model of the linear frequency synthesizer is developed and the performance at the system output is evaluated using frequency domain techniques. For a linear system, the power spectral density at the system output can be computed using known system transfer functions and known power spectral densities from the three independent noise sources: AFS, VCXO and PM. The resulting power spectral density can then be used to compute the

Allan Variance at the system output. Compared with time domain techniques, the use of frequency domain technique offers several benefits such as: (1) it provides another independent evaluation of the system performance, (2) flicker noise can be implemented precisely, (3) computation time for the Allan Variance of a given sample time ( $\tau$ ) is very short and is roughly the same for either short or long sample time ( $\tau$ ). The last two items are major drawbacks for the real-time/Monte Carlo simulations. Sensitivities of the output Allan Deviation to each of its input noises are provided, and they are valuable for design trade-off and trouble-shooting.

## 2. Noise Models

### 2.1 Phase Meter Noise

The PM noise with resolution of 100 ps is modeled as a white process with a constant power spectral density for all frequencies

$$\sigma_p(f) = \frac{(1 \times 10^{-10})^2}{6} . \quad (1)$$

And the Allan Variance of the PM noise is<sup>[1]</sup>:

$$\sigma_p^2(\tau) = \frac{(1 \times 10^{-10})^2}{6\tau^2} . \quad (2)$$

### 2.2 AFS Noise

The Allan Variances for the AFS is specified as:

$$\sigma_A^2(\tau) = \frac{9.0 \times 10^{-22}}{\tau} + 1.0 \times 10^{26} \quad (3)$$

This is consistent with that of the commercially available HP 5071 Cs AFS.

We assume that the two terms are independent of each other. Thus we can compute the associated noise power spectral densities using well known techniques<sup>[1]</sup>:

$$S_A(f) = 1.8 \times 10^{-21} + \frac{7.2134 \times 10^{-27}}{f} . \quad (4)$$

### 2.3 VCXO

The VCXO frequency noise is assumed to have the following Allan Variance:

$$\sigma_y^2(\tau) = 10^{-24} + 10^{-27} \tau . \quad (5)$$

Similarly, we assume that the two terms of equation (5) are independent of each other. As above, the power spectral density of the VCXO frequency noise can be expressed as<sup>[1]</sup>:

$$S_y(f) = \frac{7.2134 \times 10^{-25}}{|f|} + \frac{1.519 \times 10^{-28}}{f^2} \quad (6)$$

### 3. System Transfer Functions

The system model as shown in Figure 1 results in the equivalent system error model indicated in Fig. 2 obtained using the Z-transform formalism.  $T_s$  is the sample period of the system, and is 1.5 s. Also two delays of one epoch each are introduced in Figure 2 to account for the fact that the effects of the computed VCXO frequency modification in the current epoch will not show on the Phase Meter until two epochs later. The transfer functions relating the system output frequency (T) to the input noises of the AFS(A), VCXO(V) and Phase Meter (P) are:

$$\frac{\text{SYSTEMOUTPUT}}{\text{PM}} = H_{TP}(Z) = \frac{T(Z)}{P(Z)} \quad (7)$$

$$\frac{\text{SYSTEMOUTPUT}}{\text{AFS}} = H_{TA}(Z) = \frac{T(Z)}{A(Z)} \quad (8)$$

$$\frac{\text{SYSTEMOUTPUT}}{\text{VCXO}} = H_{TV}(Z) = \frac{T(Z)}{V(Z)} \quad (9)$$

The Bode Plots (frequency responses) for these second order transfer functions with a time constant of 50 s are shown in Figure 3. It is seen that  $H_{TA}(Z)$  is a lowpass filter,  $H_{TV}(Z)$  is a highpass filter, and  $H_{TP}(Z)$  is a low gain highpass filter to reduce the PM quantization noise.

### 4. Power Spectral Density of the System Output Frequency

The power spectral density of the system output ( $S_T(f)$ ) can be computed as<sup>[2]</sup>:

$$S_T(f) = S_{TA}(f) + S_{TV}(f) + S_{TF}(f) \quad (10)$$

where:

$$S_{TA}(f) = |H_{TA}(e^{j2\pi f T_s})|^2 \times S_A(f), \text{ due to the AFS noise} \quad (11)$$

$$S_{TV}(f) = |H_{TV}(e^{j2\pi f T_s})|^2 \times S_V(f), \text{ due to the VCXO noise} \quad (12)$$

and

$$S_{TF}(f) = |H_{TF}(e^{2\pi f T_s})|^2 \times S_P(f), \text{ due to the PM noise.} \quad (13)$$

The power spectral densities for the noises ( $S_A(f)$ ,  $S_V(f)$  and  $S_P(f)$ ) and their contributions to the system frequency output ( $S_{TA}(f)$ ,  $S_{TV}(f)$  and  $S_{TP}(f)$ ) were calculated using equations (1), (4), (6), (11), (12) and (13), and are shown in Figure 4. As can be seen the system output power spectral densities are shaped by their corresponding transfer functions. Even though the power spectral densities of the PM ( $S_P(f)$ ) and the VCXO ( $S_V(f)$ ) are large when compared with that of the AFS, their contributions to the system output ( $S_{TP}(f)$  and  $S_{TV}(f)$ ) have been greatly reduced by their corresponding transfer functions ( $H_{TP}(j2\pi f T_s)$  and  $H_{TV}(j2\pi f T_s)$ ) especially at low frequency. Similarly, contributions from the AFS ( $S_{TA}$ ) is also suppressed considerably for high frequencies.

## 5. Allan Deviation of the System Output Frequency

The temporal behavior of the timing or frequency system is normally characterized by the Allan Deviation or square root of the Allan Variance,  $\sigma_y^2(\tau)$ , where  $\tau$  is the frequency sample time. The Allan Variance is related to the power spectral density by [1]

$$\sigma_y^2(\tau) = 2 \int_0^{f_n} S_y(f) A_D(f\tau) df \quad (14)$$

where:

$$A_D(F\tau) = \frac{\sin^4(\pi f \tau)}{(\pi f \tau)^2} \quad (15)$$

and  $f_n$  is the Nyquist frequency of the system and is equal to 1/3 Hz for a sampling period ( $T_s$ ) of 1.5 s.

### 5.1 Computation Consideration

In many cases integration of the equation (14) can not be carried out analytically, so it must be done by computer using numerical integration. It is important to choose a proper integration step size to achieve the desired accuracy in the computation.

The magnitude of the oscillatory window function ( $A_D(f)$ ) as given in equation (15) is inversely proportional to the square of  $f$  for a given  $\tau$ , and is plotted in Figure 5 for  $\tau=100$  s and  $\tau=1000$  s. As can be seen, its magnitude decreases rapidly after a few periods and its bandwidth decreases as  $\tau$  increases. Figure 5 shows that the bandwidth is roughly  $10^{-5}$  Hz for  $\tau=1000$  s. and  $10^{-2}$  Hz for  $\tau=100$  s. The portion of the power spectral density of the system noise outside the bandwidth of the window function has negligible effect of its Allan deviation computed by using equation (14).

Given the limitations in available computer memory it was found by trial and error that to provide adequate numerical accuracy, integration of the equation (14) can be carried out by using 20 integration steps, either for the first 50 periods of the window function or up to the Nyquist frequency, whichever is smaller. This technique is valid for sample times of up to 100,000 s provided that the power spectral density function,  $S_y(f)$ , does not contain any white phase modulation noise component, whose frequency power spectral density is proportional to  $f^2$ . Fortunately this condition is met by the frequency power spectral density at the system output. For white phase modulation noise such as the PM noise, the upper limit of the numerical integration has to be set at the Nyquist frequency. For larger sample times,  $\tau > 100,000$  s, a smaller integration step size is needed. The average time to compute the Allan Deviation for a given  $\tau$  is less than 15 s using a PC with Intel 486 DX2/50 CPU.

To show that this numerical integration technique is accurate enough the Allan Deviations of the two noise sources (AFS and VCXO) are computed from their corresponding power spectral densities using equation (14) and are shown in Figure 6. Figure 6 also shows the corresponding specified Allan Deviations, from which the power spectral densities were derived, as discussed in section 2. As can be expected, the computations are in very good agreement with the respective specifications. The Allan Deviation of the PM noise is also depicted. Figure 6 shows that the PM Allan Deviation is predominant for sample times up to 30 s and that of the VCXO noise predominates for longer time.

## 5.2 System Allan Deviation

The contribution to the Allan Deviations at the system output ( $\sigma_{TA}(\tau)$ ,  $\sigma_{TP}(\tau)$  and  $\sigma_{TV}(\tau)$ ) due to each of the independent input noises are computed using equation (14) with their power spectral densities at the system output ( $S_{TA}(f)$ ,  $S_{TP}(f)$ , and  $S_{TV}(f)$ ). The results are shown in Figure 7 and they can be considered as the sensitivities of the system output for each of the input noises. This technique can be used very effectively during the design, development and testing phase of the system to determine the loop time-constant, to define noise specifications and to provide data for trouble-shooting. It will be used below to identify the causes of some exceeding reference AFS specification conditions. It is apparent from Figure 8 that for short sample time the system performance is dominated by the PM, while for long sample time the system performance is governed by the AFS. The crossover sample time is around 20 s. The Allan Variance of the resulting system output can be obtained as:

$$\sigma_T^2(\tau) = \sigma_{TA}^2(\tau) + \sigma_{TV}^2(\tau) + \sigma_{TP}^2(\tau). \quad (16)$$

The Allan Deviations of the system output ( $\sigma_T(\tau)$ ) and the reference AFS specification are plotted in Figures 8. Figure 8 shows that the Allan Deviation of the system output barely exceeds the reference AFS specification for sample time from 70 s to 1000 s. By examining the system sensitivities as provided in Figure 7, it is found that this condition is caused by the AFS noise.

## 6. System Performance Using Other System Configurations

In the previous sections we only use  $T_c = 50$  s, Allan Deviation results using other time constants can be obtained easily. The result for a time constants of 15 s is shown in Figures 9. Figure 9 indicates that the system exceeds the reference AFS Allan Deviation specification for  $\tau = 1000$  s. The cause can be determined by examining the sensitivities as shown in Figure 10, and is identified to be the PM noise, which is the dominant noise contribution for short  $\tau$ ; its effect at the system output is not suppressed enough for the system with a short time constant. To reduce the effect due to the PM for short sample time, a better PM with resolution of 20 ps was used and the result is shown in Figure 11. As can be seen the Allan Deviation at the system output is less than that of the reference AFS for short sample time.

## 7. Conclusion

An efficient method of computing the Allan Deviation at the output of a linear system with known input power spectral densities is presented. Since the computation time is not a function of the sample time ( $\tau$ ), this technique is very attractive to compute Allan Deviations for long sample times. Sensitivities of the Allan Deviation at the system output for each of its independent input noises are also provided and they are valuable for design trade-off and trouble-shooting. Potential situations in which the system could exceed the reference AFS specification are pointed out, and causes are identified.

### References

- [1] J. Barnes, Andrew R. Chi, Leonard S. Cutler, Daniel B. Leeson, Thomas E. McGunigal, James A. Mullen, Jr., Warren L. Smith, Richard L. Sydnor, Robert F. C. Vesot, and Gernot M. R. Winkler, "Characterization of Frequency Stability," IEEE Trans. Instrumentation and Measurement, IM-20, May 1971.
- [2] A. Papoulis, "Probability, Random Variables, and Stochastic Processes," McGraw-Hill, New York, 1965.

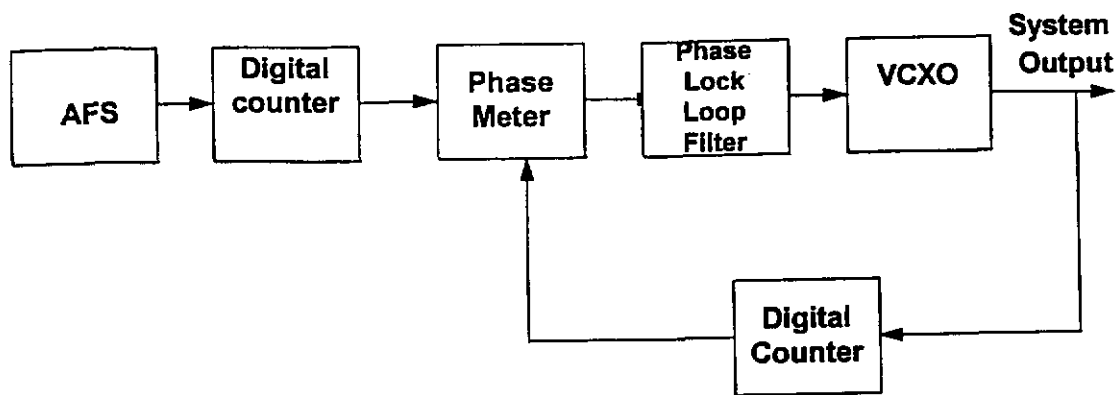


Figure 1. Linear Frequency Synthesizer

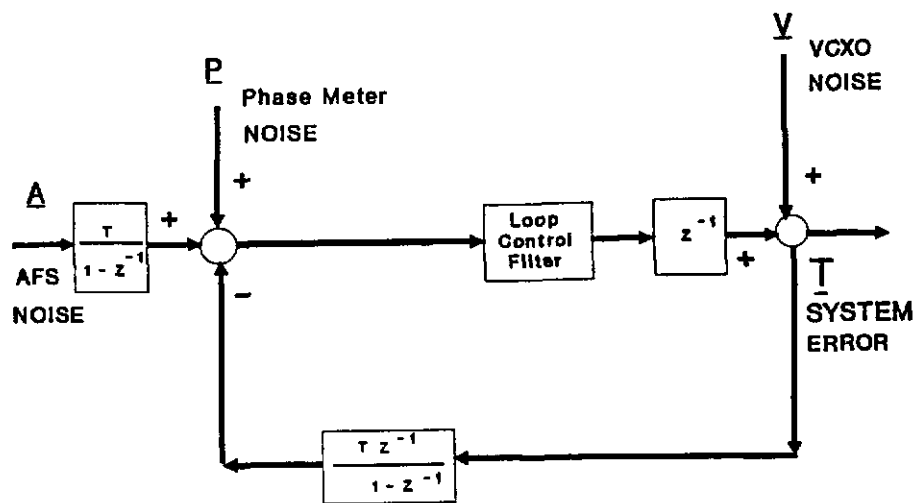


Figure 2. System Error Model

Fig. 3. Bode Plots of System Transfer Functions

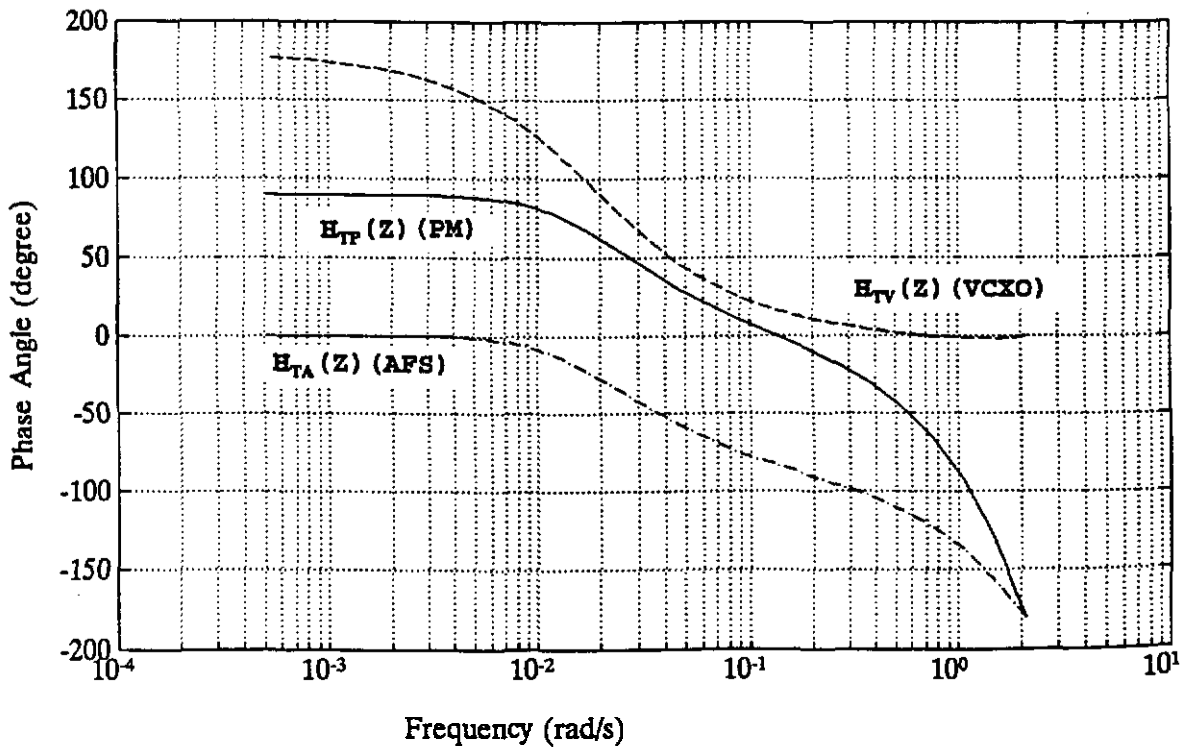
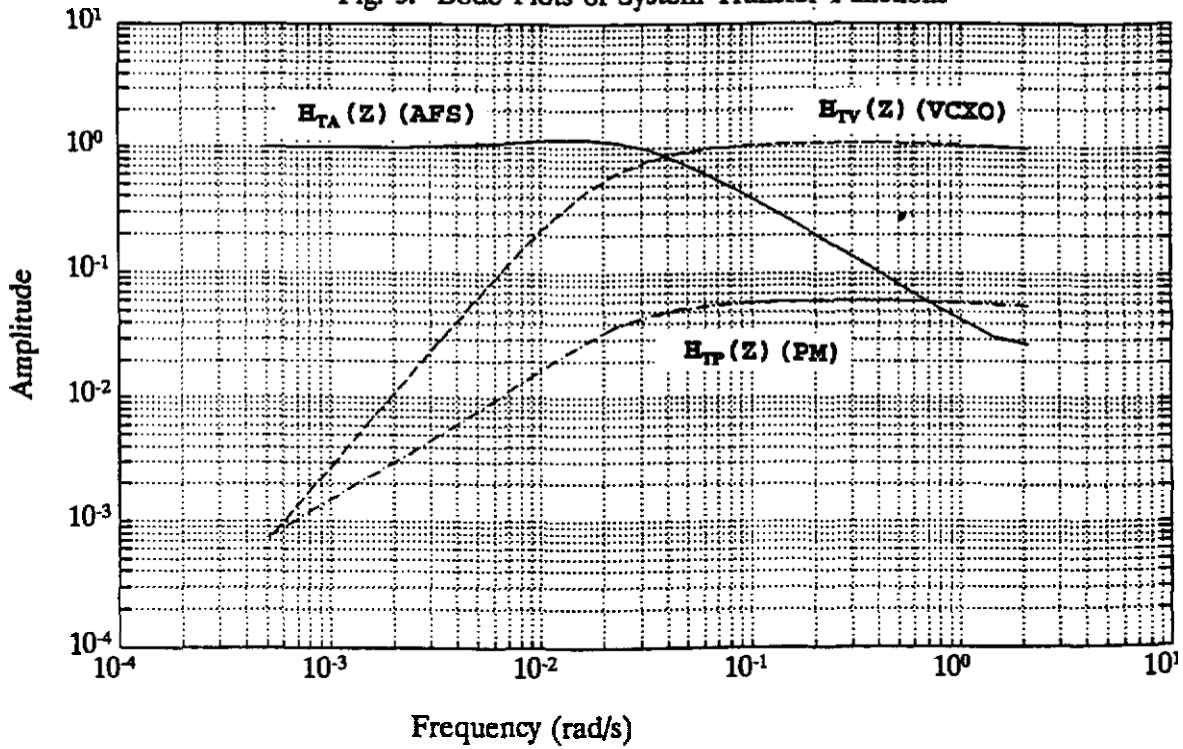




Figure 4. Power Spectral Densities of PM, VCXO and AFS

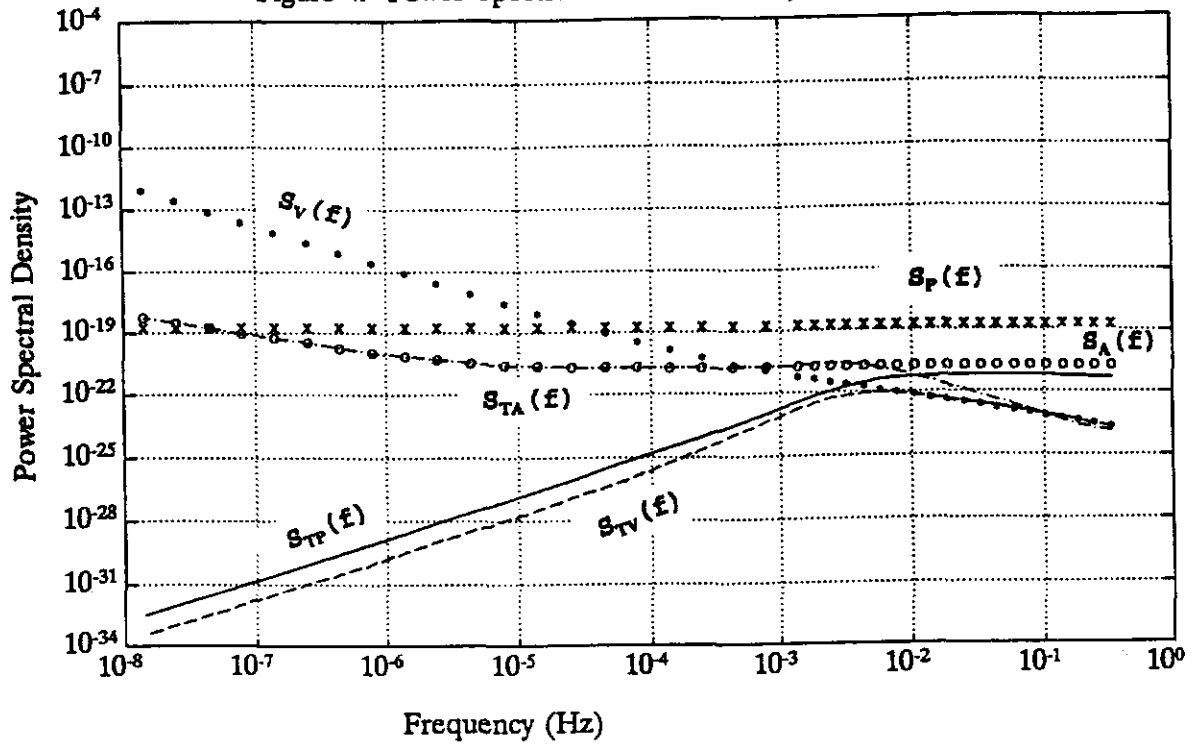


Figure 5. Plot of Window Function as functions of  $f$  and  $\tau$

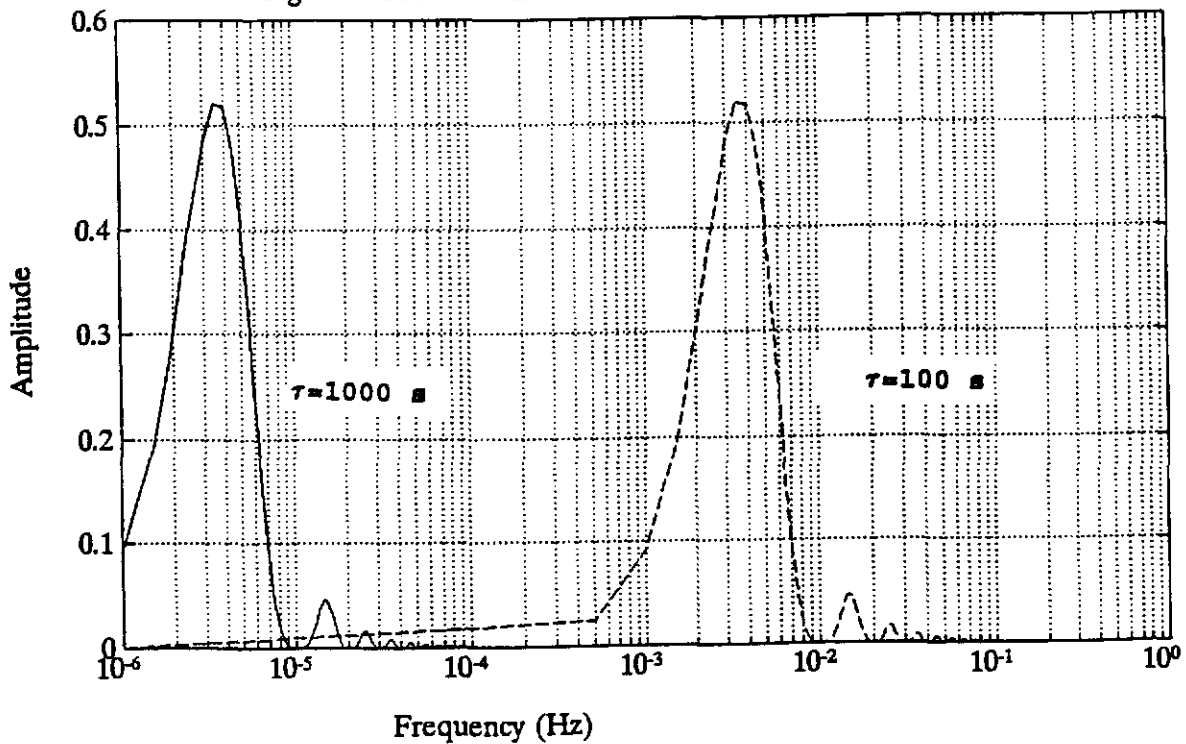


Figure 6. Allan Deviations of PM, VCXO and AFS

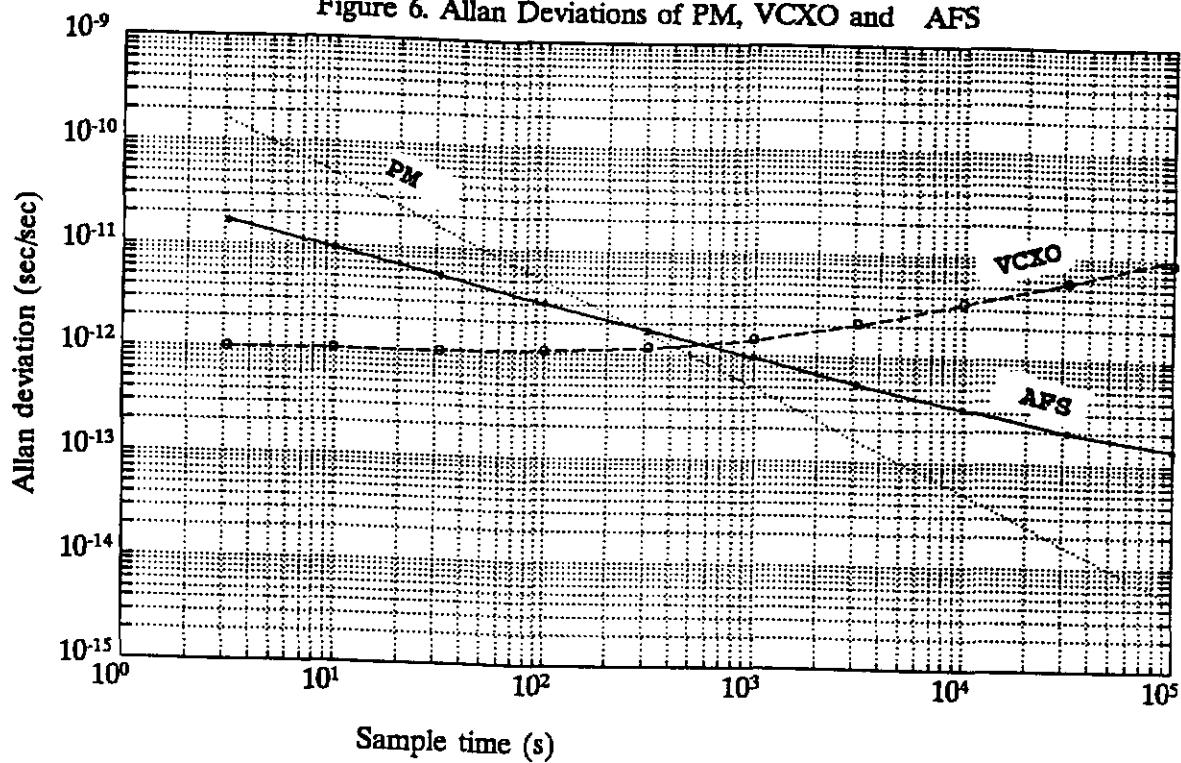


Figure 7. System Sensitivities

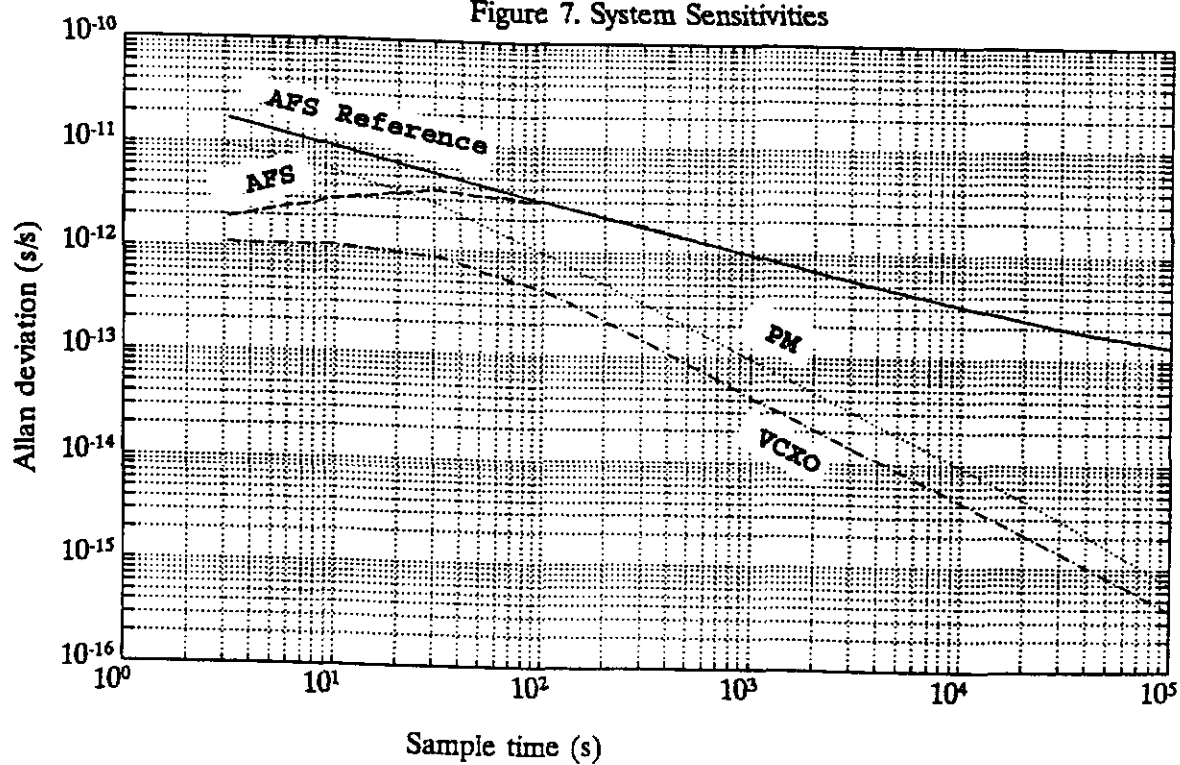


Figure 8. AFS Reference & System Output Allan Deviations

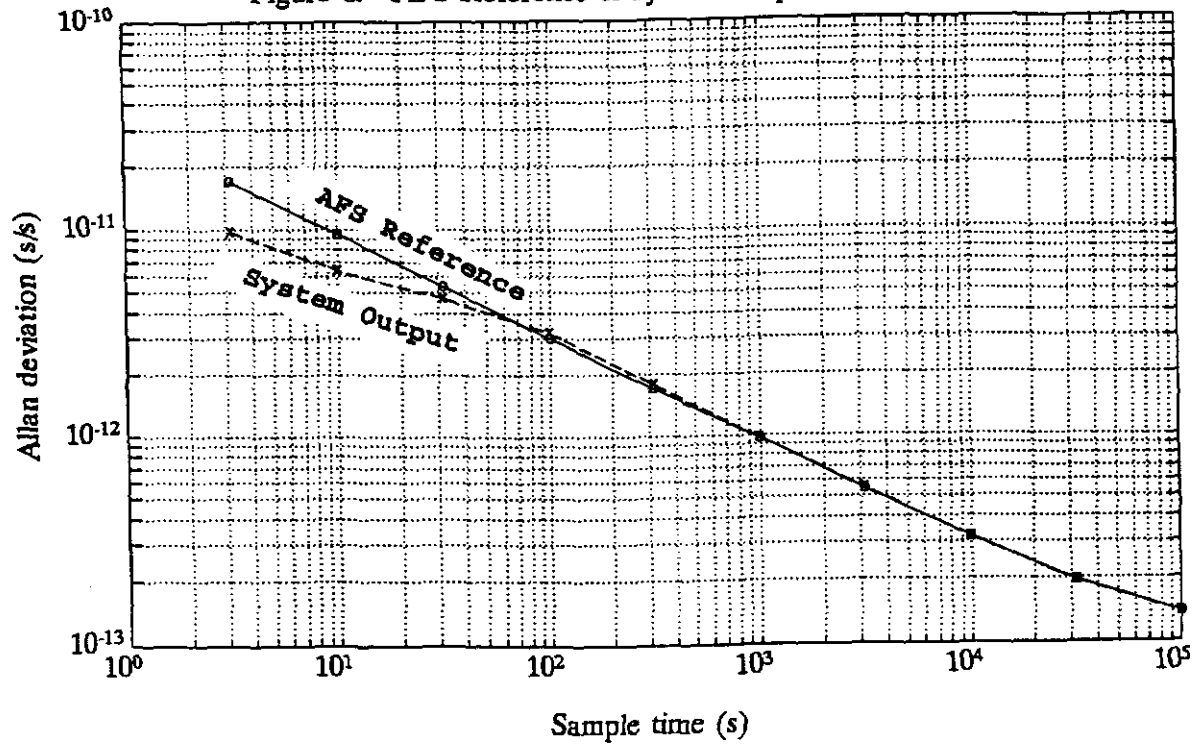


Figure 9. System Output Allan Deviation for  $T_c=15$  s

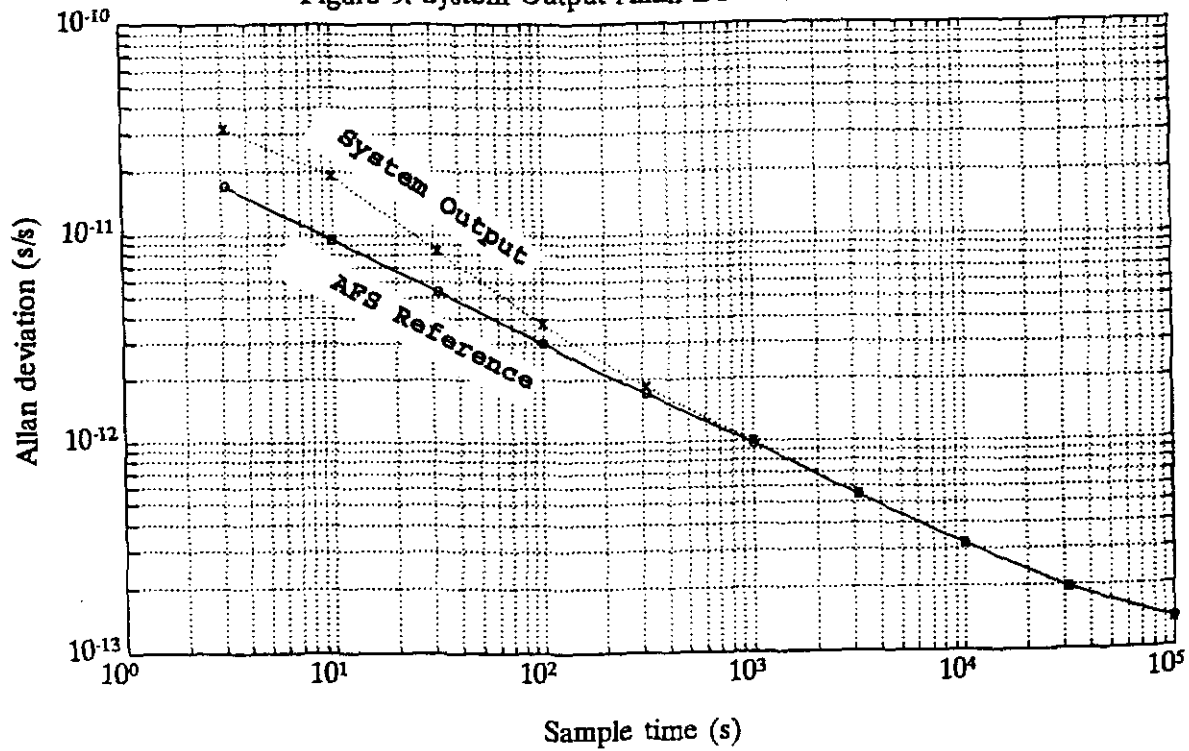


Figure 10. System Sensitivities for  $T_c=15$  s

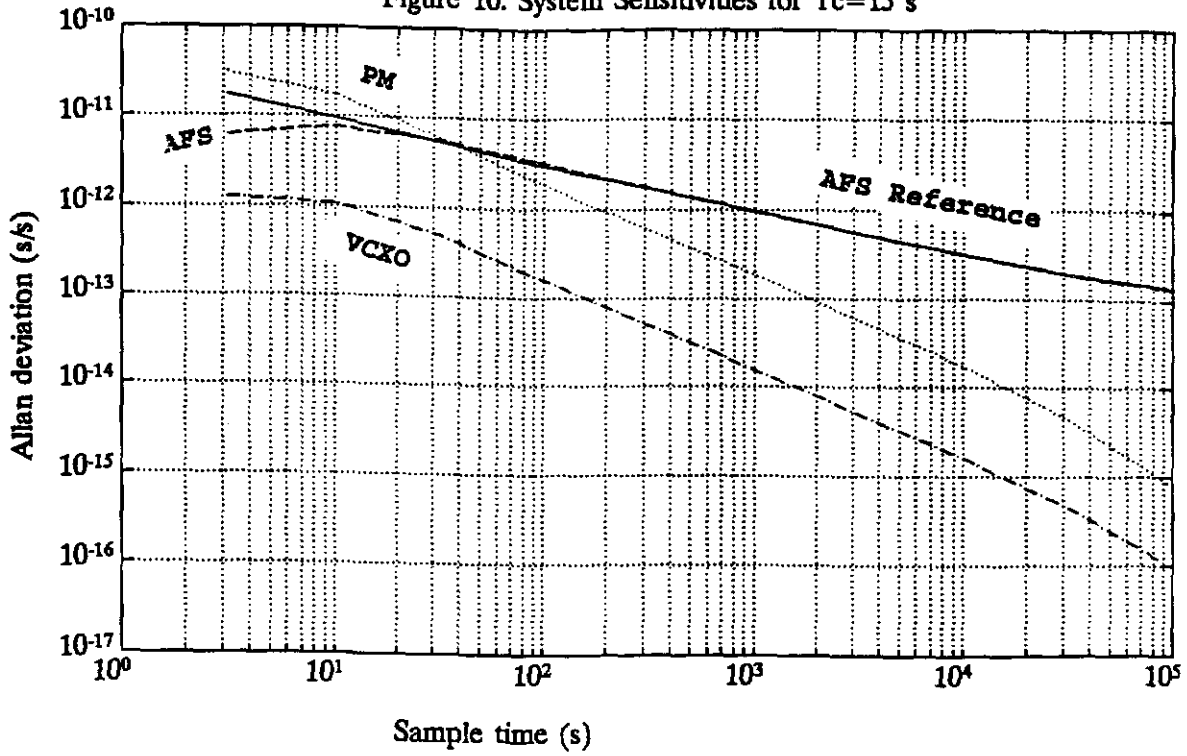


Figure 11. System Output Allan Deviation for Better PM

